PERGAMON

Progress in Surface Science 64 (2000) 179–191

Progress in SURFACE SCIENCE

www.elsevier.com/locate/progsurf

Tip–surface interactions in noncontact atomic force microscopy on reactive surfaces

I. Štich[a,*], J. Tóbik[a], R. Pérez[b], K. Terakura[c,d], S.H. Ke[c,d]

[a]*Department of Physics, Slovak Technical University (FEI STU), Ilkovičova 3, 812 19, Bratislava, Slovakia*

[b]*Departamento de Física Teórica de la Materia Condensada, Universidad Autónoma de Madrid, E-28049, Madrid, Spain*

[c]*JRCAT, National Institute for Advanced Interdisciplinary Research, 1-1-4 Higashi, Ibaraki 305-8562, Tsukuba, Japan*

[d]*Institute of Industrial Science, University of Tokyo, Roppongi, Minato-ku, Tokyo, 106-8558, Japan*

Abstract

The imaging process in noncontact atomic force microscopy (AFM) is studied on a number of reactive surfaces, namely, the Takayanagi reconstructed Si(111), InP(110), and GaAs(110). We show that on these surfaces, the short-range dangling-bond type of interaction between the tip and the surface is decisive in achieving atomic resolution. The short-range tip–surface interaction is modeled in the density functional theory within the GGA approximation. We show that we can achieve quantitative agreement with the experimental data in the commonly used frequency modulation technique for AFM surface corrugation with a very simple model for the tip geometry treating the tip–surface interaction in the perturbation theory. The nature of the short-range tip–surface interaction on the three surfaces is considered and the consequences thereof for the experiments is discussed.

1. Introduction

The *atomic force microscope* (AFM) [1] has developed as a tool which allows

* Corresponding author.

0079-6816/00/$ - see front matter
PII: S0079-6816(00)00015-0

routine investigation of surface structures. The apparatus measures spatial variations of the forces between a tip and a surface. The atomic forces between the tip and the surface should, at least in principle, be more directly related to the surface atomic structure than is the case in the *scanning tunneling microscopy* (STM), which is probing the electronic band structure around the Fermi level. However, the images taken in the contact mode were not capable of achieving atomic resolution.

The breakthrough came only recently when the capability of the AFM operating in a noncontact regime in UHV [2,3] was demonstrated on reactive surfaces. In its original version, the *frequency shift mode* [4], the frequency of a tip oscillating at its eigenfrequency ω is modified by an amount $\Delta\omega$ as a result of the change of the cantilever spring constant k by Δk due to the tip surface interaction

$$\frac{\Delta\omega}{\omega} \propto \frac{\Delta k}{k}. \tag{1}$$

The images are taken at a constant $\Delta\omega$ by adjusting the sample height. Recently, alternative methods, such as amplitude damping or constant excitation mode [5] have been introduced to produce images of reactive surfaces with atomic resolution. These are somewhat less directly related to our theoretical analyses and will not be discussed here. The question, however, remains as to how the topographs so collected, correspond to the surface structure. It is the principal objective of this paper to demonstrate that the first-principles modeling is an indispensable tool in this respect.

The rest of the paper is organized as follows. In the next section we analyze the possible ways to simulate the AFM images produced by operating in a noncontact frequency modulation mode and discuss the theoretical modeling of the tip–surface forces. In Section 3 we apply the tools developed in the previous sections to three reactive surfaces: the Takayanagi reconstructed Si(111) surface; and (110) surfaces of InP and GaAs.

2. Simulation of AFM images and the nature of tip–surface forces

In order to simulate the AFM image one has to have the dependence of $\Delta\omega$ in (1) on some physical quantity sensitive to the atomic surface structure. The first proposal was to assume that $\Delta\omega$ is proportional to the gradients of the tip–surface force

$$\Delta\omega \propto \frac{\partial F_{\text{tip-sample}}}{\partial z}. \tag{2}$$

However, this has been shown not to be valid.

A more realistic approach is to use the *classical perturbation theory* [6,7], which is based on canonical transformations using the method of generating functions. The goal is to find the coordinate system (w, J), where the Hamiltonian is a

function of only the canonical momentum, which is attainable for systems with a known solution. The cantilever dynamics are described by the Hamiltonian

$$H = \frac{p^2}{2m} + k\frac{q^2}{2} + V_{\mathrm{p}}(q) = E. \tag{3}$$

The (w, J) coordinate system, without the perturbing term V_{p}, has the form:

$$w_0 = \nu_0 t, \quad J_0 = \frac{E_0}{\nu_0}, \quad H_0 = J_0\nu_0,$$

$$q_0 = \sqrt{\frac{J_0}{2\pi^2 m\nu_0}}\,\sin(2\pi w_0), \quad p_0 = \sqrt{2m\nu_0 J_0}\,\cos(2\pi w_0). \tag{4}$$

The transformation between the two coordinate systems, which preserves the form of the Hamiltonian, is obtained by the generating-function (GF) method. For a generating function F, the old and new coordinate systems are related via:

$$p = \frac{\partial F}{\partial q}, \quad w = \frac{\partial F}{\partial J}, \quad H = K - \frac{\partial F}{\partial t}. \tag{5}$$

The analytic form of the *generating function* (GF) can be found by solving the Hamilton–Jacobi equation $H(q, \partial F/\partial q) = E$. The advantage of the GF method is that the system with a small change of the Hamiltonian can be solved perturbatively. Assume that, for a small change of the Hamiltonian, the change of the GF will also be small, the GF and the Hamiltonian can be expanded in powers of a small parameter ε, i.e.,

$$H(w_0, J_0) = H_0(J_0) + \varepsilon V_{\mathrm{p}}(w_0, J_0) = E_0 + \varepsilon E_1,$$

$$F = F_0 + \varepsilon F_1(w_0, J) = w_0 J + \varepsilon F_1(w_0, J). \tag{6}$$

Using relations (5) we find:

$$V_{\mathrm{p}}(w_0, J) + \frac{\partial H_0}{\partial J}\,\frac{\partial F_1(w_0, J)}{\partial w_0} = E_1. \tag{7}$$

It can be proved [7] that the second term on the left-hand-side vanishes by integration over one oscillation period. Hence, the first correction to the energy is given by $E_1 = V_{\mathrm{p}}$. The final relation for the frequency shift therefore reads:

$$\Delta\nu \approx \frac{\partial E_1}{\partial J} = \frac{\partial \bar{V}_{\mathrm{p}}}{\partial J_0} = \frac{\partial}{\partial J_0}\,\frac{1}{T}\int_0^T V(q(t))\mathrm{d}t. \tag{8}$$

Note, that the last equation is very similar to the earlier proposition (2), assuming that the frequency shift is proportional to the force gradient. There is, however, a

small difference in that the average of the perturbation must be taken over the whole path and not only at the end point.

In order to use (8), the tip–surface force must be modeled on a dense grid of points in a surface unit cell. Integrating these functions leads to the perturbing potential $V_p(d)$, for the vertical motion of the tip, which is expressed in the q coordinate system by a transformation that depends on Δ, the distance between the substrate surface and the tip equilibrium position (Fig. 1). Therefore, $V_p(q)$ in (3) is given by $V_p(q) = V_{int}(\Delta - q)$. The frequency shift can then be determined as a function of d_{min}, defined as the shortest distance between the tip and the surface during the whole trajectory of the tip. The other parameters, which enter the calculation, can be taken from the experiments. Finally, since the motion of the cantilever is one-dimensional, it can also be directly modeled, once the tip–surface interaction is known.

The ability to simulate the AFM images critically depends on the ability to accurately model the tip–surface interactions, which is a complicated problem, as the nature of the force varies with the tip–surface distance z. At large separations, the tip–surface interaction will be dominated by the *Van der Waals* (VdW) forces, while at small separations the short-range quantum–chemical forces will be dominant. It has been shown [8,9] that the latter contribution can reliably be modeled via the *density functional theory* (DFT). On the other hand, a standard DFT theory for VdW interactions has not yet been developed. For this reason, we use the *Hamaker summation method* to model the VdW component [10]. More importantly, it has been shown theoretically [8,9], as well as experimentally [5,11,12], that on reactive semiconductor surfaces the chemical interactions are responsible for the atomic resolution. All the technical details are given elsewhere [8,9,13,14], so here only a very brief characterization of the technical details of the DFT modeling of the chemical interactions is provided. These are computed by making stepwise small movements in the vertical direction. The main ingredients are as follows: DFT in plane-wave pseudopotential formalism [15]; *generalized*

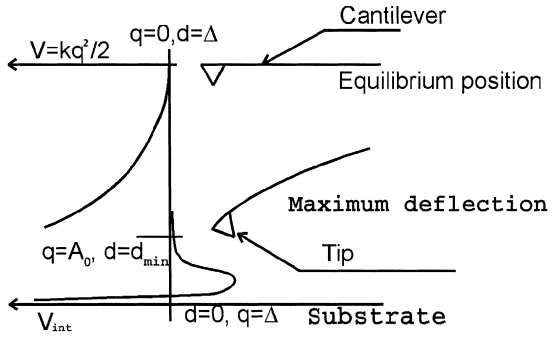

Fig. 1. Schematics for FM-AFM experiments. The spring and tip–surface potentials are on the left. The relation between q, d and Δ is given by equation $d+q=\Delta$. Δ changes so slowly, it can be considered constant during one period.

gradient approximation (GGA) to the exchange–correlation functional in the PW91 form [16]; 8Ryd plane-wave cutoff; Γ-point sampling of the Brillouin zone; slab geometry for the surface; highly accurate computation of the extremely small tip–surface forces ($\Delta \mid \mathbf{F} \mid \sim 1 \times 10^{-2}$ nN).

The models for the tips require a special consideration. Si-tips are modeled since they were used in all the experiments [5,11,17,18]. The three tip models [9,8] in Fig. 2 were carefully tested. They differ in size (four-atom and 10-atom tips) and in the presence or absence of the tip base saturation by hydrogen, which produces a dangling bond sticking out of the tip apex atom. The presence/absence of this dangling bond causes dramatic changes in the short-range interaction results, which, on the reactive surfaces, are totally dominated by the dangling-bond type of interaction. The role of the tip size is much less important. Unless stated otherwise, results have been obtained with the 10-atom tip with an H-saturated base.

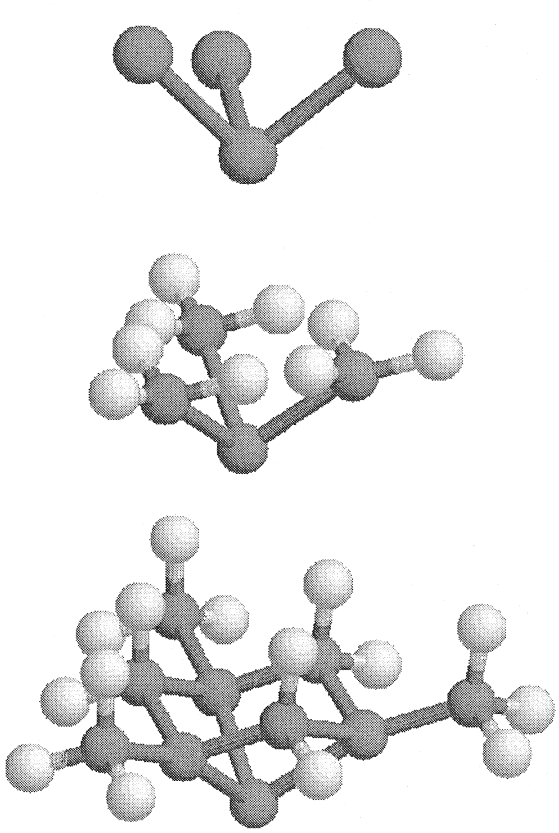

Fig. 2. Ball and stick models of tips used in simulations.

3. Results

3.1. Si(111) surface

The experimentally observed reconstruction of the Takayanagi reconstructed Si(111) surface has a 7×7 unit cell, which is too large for *ab initio* modeling at the required level of accuracy. For this reason, the surface is modeled by a 5×5 reconstruction, which is the smallest member of the family having all the relevant ingredients, namely, adatoms and rest atoms, as well as dimers and a stacking fault over one-half of the unit cell. The top view of the model is shown in Fig. 3.

The results of the computed total energies and forces, due to short-range interactions over different sites in the unit cell, are shown in Fig. 4. Despite the dangling-bond type of interaction between the tip and the surface atom the curves have a rather complicated shape, which cannot be fitted easily with simple analytical forms, such as the Morse potential. This is due to the fact that there is a very significant relaxation process at both the tip apex atom and the surface atoms. Otherwise, the different curves are of similar shape, and the shifts are primarily due to the different heights of the atoms on the surface.

The calculated tip–surface interaction, together with some experimental parameters [11], were used in the perturbation theory. The VdW component, treated in the Hamaker summation method [10], was added by considering a sphere of radius 40 Å interacting with a flat Si surface. In this model, using the experimental parameters, the AFM height of the adatom was found to be ~3.4 Å and for the corner holt atom ~2.05 Å (Fig. 4), which gives a computed

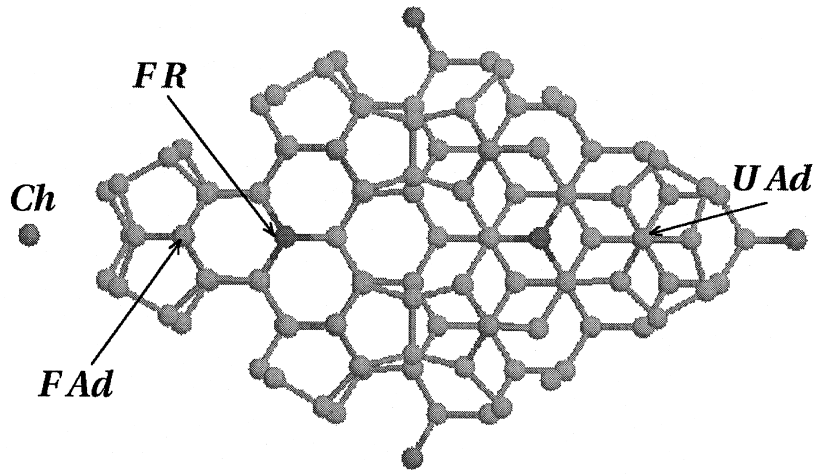

Fig. 3. Top view of model Si(111) 5×5 surface. The positions of various types of surface atoms are marked. *FR* — faulted rest atom, *U*/*F* Ad — unfaulted/faulted adatom, *Ch* — corner hole.

corrugation between the adatom and corner hole atom ~1.35 Å, in reasonable agreement with the experimental value of ~1.7 Å.

Because of the large computational cost of the *ab initio* treatment, the entire computed AFM image of the unit cell could not be generated for comparison with

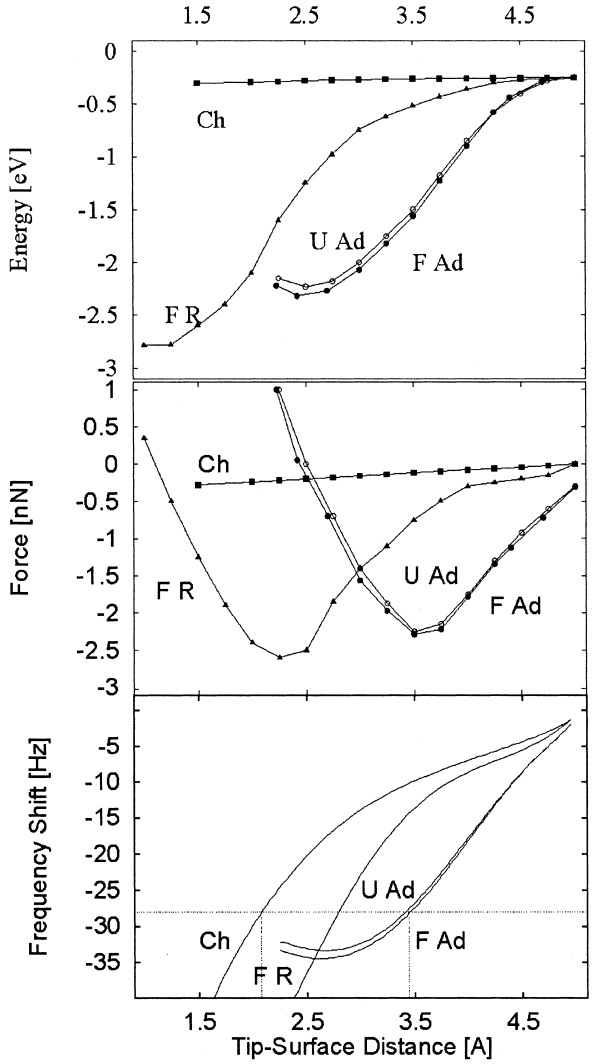

Fig. 4. Energy (top panel), normal force (middle panel) and frequency shift (bottom panel) dependence on tip–surface distance for various types of the Si(111) 5 × 5 surface atoms. Oscillator parameters (spring constant k = 41 N/m, maximum amplitude A_0 = 164 Å, basic frequency ν_0 = 172 kHz, frequency shift $\Delta\nu = -28$ Hz) were taken from the experiment [11]. Note the approximate VdW component was added to short-range interactions (cf text).

the experiments. A quick qualitative insight into the AFM image is provided by lateral scans along the long diagonal in the surface unit cell with the tip at a distance of 5 Å. Deep minima in both the energy and force curves were found with the rest of the atoms being barely visible in the force curves, in qualitative agreement with the experimental results showing, essentially, only the images of the adatoms [2].

Analysis suggests that the AFM image arises from "local reactivity" between the tip and the surface. Hence, the image is *not* a genuine property of the surface, since the experimental image also depends on the tip, as verified experimentally. The corrugation obtained with an Si tip follows the decreasing order [11]: $Co{-}F > Ce{-}F > Co{-}U > Ce{-}U$, while for a W tip [12]: $Ce{-}F > Ce{-}U > Co{-}F > Co{-}U$, with *Co* (*Ce*) standing for the *corner* (*center*) adatom and *U* (*F*) for the *unfaulted* (*faulted*) half of the unit cell.

3.2. InP(110), GaAs(110) surface

Both surfaces have been imaged recently [17,18,5], the result showing only one (anion) sublattice, which raises the question as to why this happens. The ball and stick model of the InP(110) surface with the tip used in our calculations is shown in Fig. 5. There are some important differences with respect to the Si(111) surface. Firstly, the surface atoms carrying the dangling bonds on the III–V surfaces, which retain the 1×1 symmetry, are much closer to each other compared to the Si(111) surface, where the adatoms are locally arranged in a 2×2 configuration. Hence, more complicated multi-bond configurations between the tip and surface may arise. Secondly, as a result of surface relaxation, important rearrangements occur in that the surface atoms adopt an sp^2 hybridization with the anion moving outwards and cation moving inwards. One can expect this type of hybridization to be more susceptible to tip perturbation than was the case on the Takayanagi reconstructed Si(111) surface.

The calculated displacement curves over the P and In atoms are shown in Fig. 6. At short distances, a very significant surface response, leading to a complicated medium range tip-induced surface relaxation, occurs over both ions. Surprisingly, the minima of the force curves over both atoms are very close to each other, despite the surface buckling of the clean surface being 0.645 Å. This occurs because the P atom relaxes inwards in response to the tip, whereas the In atom does not. In addition, over the In atom, around $d \approx 2$ Å, an onset of a large lateral force on the tip apex occurs, which significantly modifies the tip structure. Basically, around this distance the tip–dangling bond starts forming a bond to one of the nearby P atoms, whose force is clearly reflected in the energy and force curves.

The vertical part of the computed force displacement curves was used in the perturbation theory. Utilizing the experimental parameters, $d_{\min}$ is $\sim$3.3 and $\sim$3.0 Å over the P and In atom, respectively. From these numbers, a surface corrugation of $\approx$0.3 Å is estimated, which is in good agreement with the value of the corrugation of 0.19 ± 0.05 and 0.12 ± 0.05 Å for [001] and $[1\bar{1}0]$ direction,

respectively [17]. The latter value is more relevant. Results in good agreement with the experiments were obtained using only the short-range part of the tip–surface interaction, which points to the fact that a very sharp tip must have been used in the experiment [17]. Obviously, adding the VdW component could lead to even better and more quantitative agreement with the experimental result.

Given the close similarity between the InP and GaAs(110) surfaces, as well as between their AFM images, it could be concluded that the tip–surface interactions must also be very similar on the two surfaces. From the results for the GaAs surface in Fig. 8, it is clear that this is *not* the case. For the Ga atom, a complicated hysteretic behavior occurs due to the softness of the *potential energy surface* (PES). The spring constant of the Ga atom is exceeded and the atom moves between two minima on the PES. Similarly, for the As atom multi-minima curves were found, whose details are explained elsewhere [14]. The reason why the AFM images show such a striking similarity between the two surfaces has to do with the fact that the experiments are performed at distances with no large differences in the PES. If the experiments could be done at smaller tip–surface distances, pronounced differences would be expected.

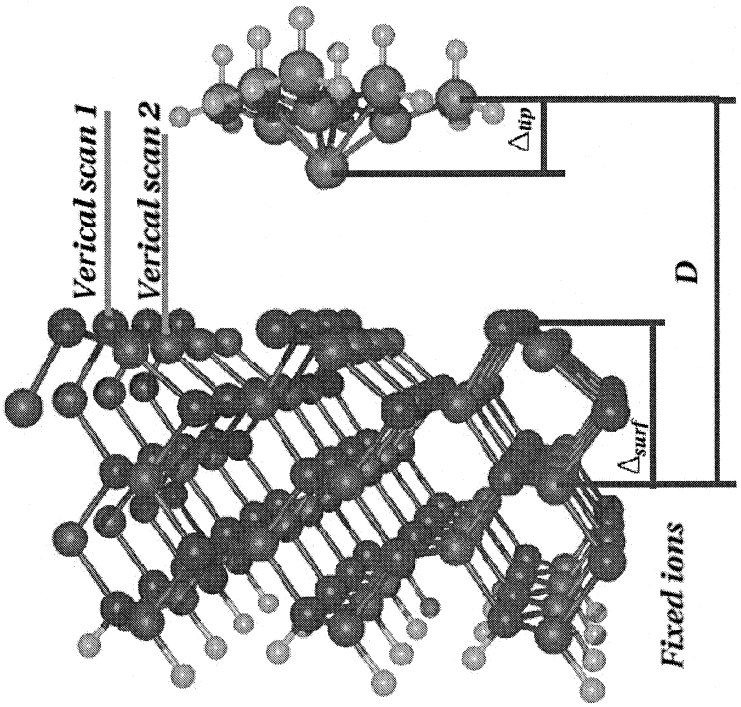

Fig. 5. Simulation geometry. Tip–surface distance is defined as $d = D - \Delta_{tip} - \Delta_{surf}$, where Δ_{tip}, Δ_{surf} are taken before mutual tip–surface interaction is switched on. P atoms are outermost atoms on the surface.

Finally, the lateral scans for the InP(110) surface are shown in Fig. 7, where only the anion sublattice can, indeed, be experimentally observed. There is no corrugation along the In atoms (cf Fig. 7,), despite the fact that the magnitude of the force in that direction is comparable to that over the P atoms. This is because of the sp^2 hybridization, which makes the dangling bonds on the anion (cation)

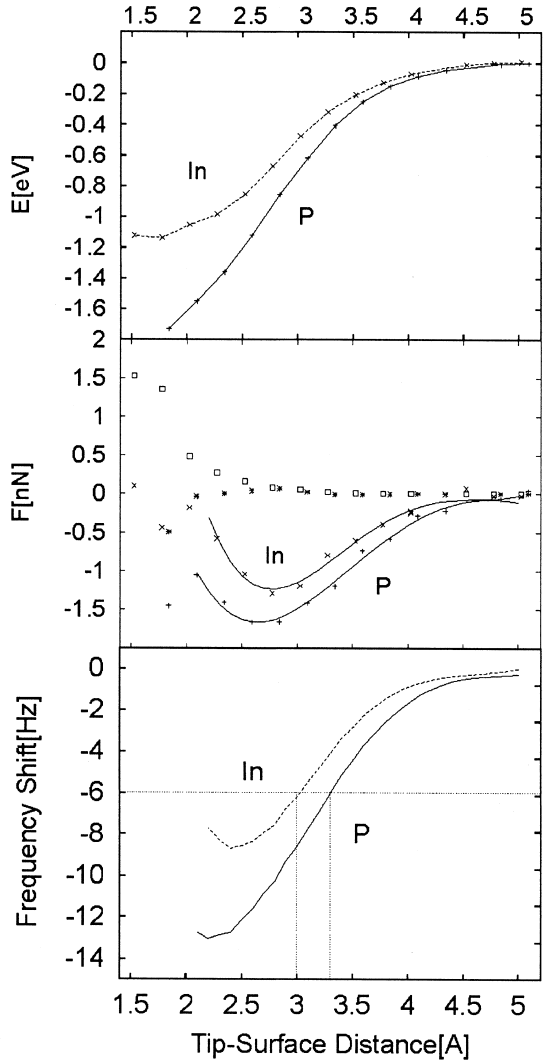

Fig. 6. Displacement curves for InP(110) surface and Si-tip. The top panel shows total energy change; middle panel normal (diamonds, pluses) and lateral (crosses, squares) parts of tip–surface force over both types of surface atoms. The bottom panel shows calculated frequency shift. Other parameters were taken from the experiment [17] ($\nu_0 = 151$ kHz, $k = 34$ N/m, $A_0 = 200$ Å and $\Delta\nu = -6$ Hz).

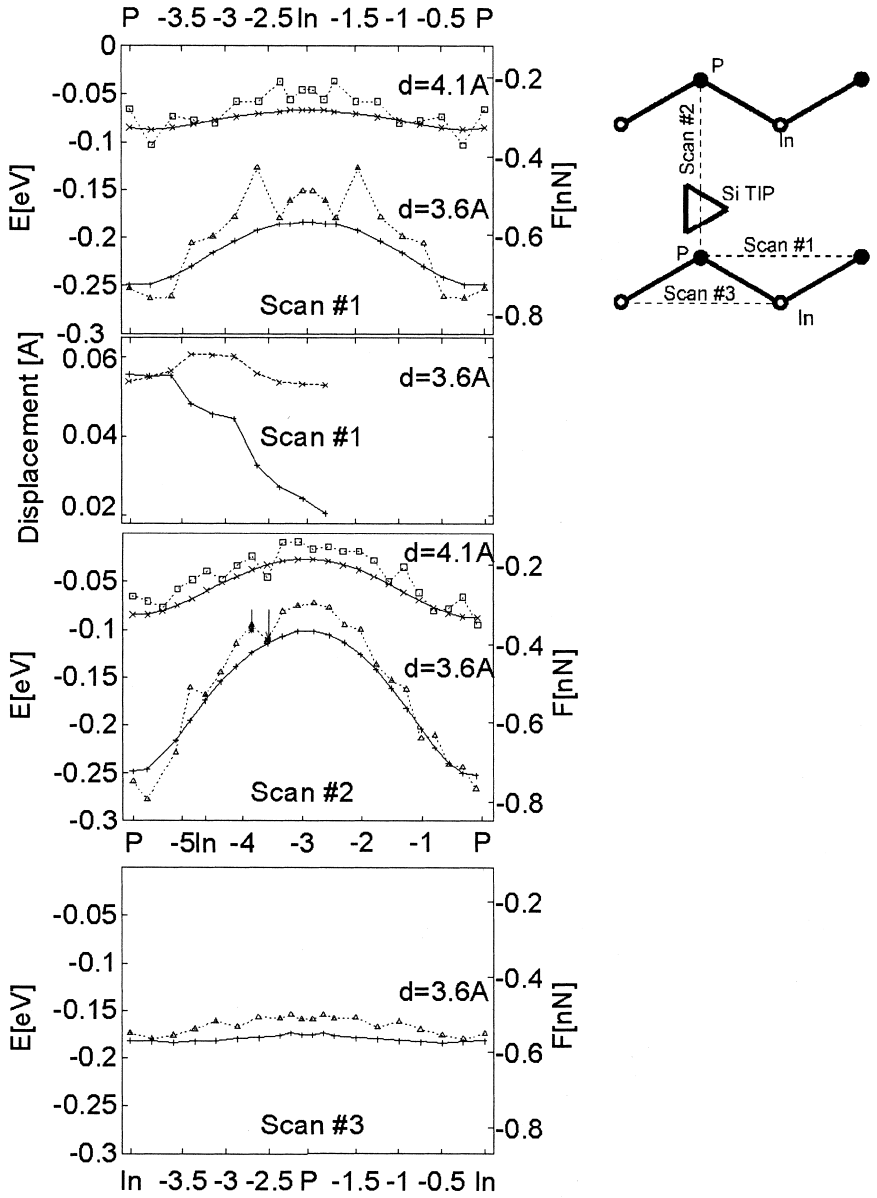

Fig. 7. Short-range interaction energy (full lines) and normal tip–surface force (dotted lines) for lateral scans with tip scanning at tip–surface distance d indicated in the panels. Positions of the atoms on the scan axis and nearby off-axis atoms are also shown. For scan No. 1, the second panel from the top depicts the total displacements (in Å) of two surface In atoms, showing discontinuities in their relaxation pattern. In scan No. 2, arrows indicate two points recalculated by bringing the pristine tip and surface to the distance of 3.6 Å.

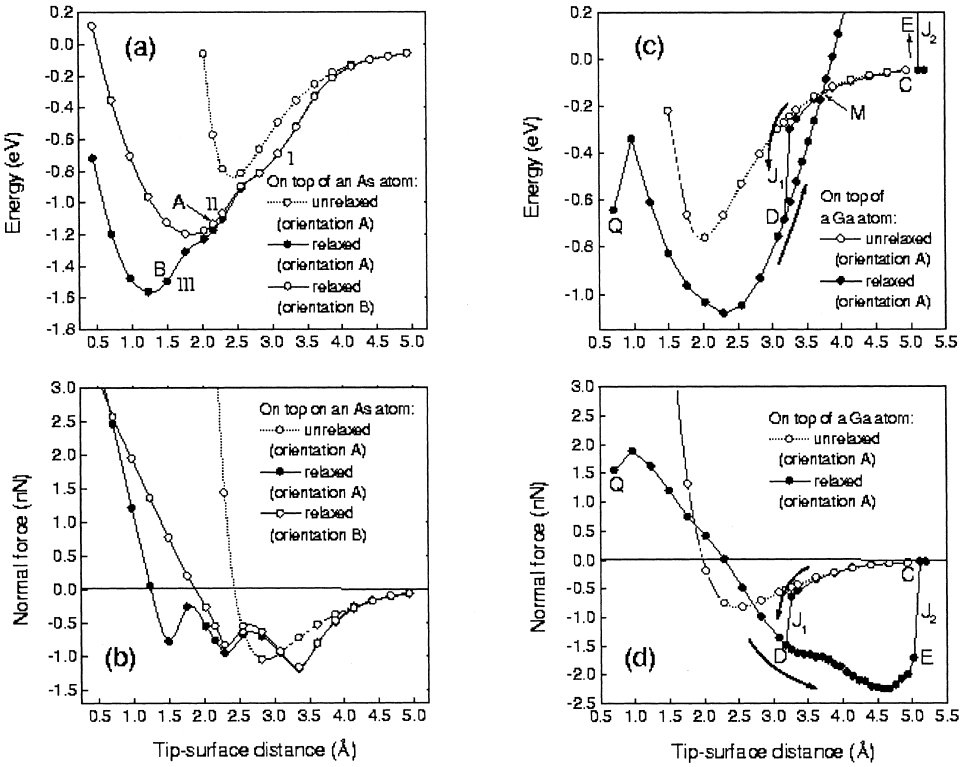

Fig. 8. Displacement curves for GaAs(110) surface. Hysteretic behavior of the tip and surface deformation is marked by arrows. The two tip orientations correspond to different multibond tip–surface interactions.

atoms occupied (unoccupied), and hence, visible (invisible) to the tip. The "spiky" shape of the force curves is caused by discontinuities in the lateral relaxation of some surface atoms, which move discontinuously over the barriers separating the minima on the PES as the tip base is moved (Fig. 8).

4. Conclusions

It has been shown how *ab initio* total-energy techniques can be used to study the atomic resolution of the non-contact AFM on reactive surfaces. The results indicate that, for this class of surfaces, relatively simple models for the tip–surface interaction, combined with the perturbation theory, can lead to qualitatively correct results.

The picture emerges that it is the short-range chemical type of interaction, which significantly enhances the atomic resolution of the AFM on reactive

surfaces. It would also be very interesting to understand the recent experiments demonstrating atomic resolution on metallic surfaces [5], where undoubtedly, the mechanism leading to atomic resolution will be different from the one we have identified here. The other conclusion is that, due to the complexity of the tip–surface interaction, the interpretation of the experimental AFM images may be as complicated as in the STM. Hence, as in STM, theory may play a significant role in understanding the experimental images.

Acknowledgements

The calculations were performed on the JRCAT supercomputer system. This work was partly supported by the New Energy and Industrial Technology Development Organization (NEDO). I.S. thanks JRCAT and the Atom Technology Partnership for a Collaborative Research Project award. R.P. acknowledges financial support from the CICyT (Spain) under Contract PB97-0028.

References

[1] G. Binnig, C.F. Quate, Ch Gerber, Phys. Rev. Lett. 56 (1986) 930.
[2] F.J. Giessibl, Science 267 (1995) 68.
[3] S. Kitamura, M. Iwatsuki, Jpn J. Appl. Phys. 35 (1995) L145.
[4] T.R. Albrecht, P. Grütter, D. Horne, D. Rugar, J. Appl. Phys. 69 (1991) 668.
[5] Appl. Surf. Sci. 140 (1999) Issues 3–4.
[6] F.J. Giessibl, Phys. Rev. B56 (1997) 16,010.
[7] W. Dittrich, M. Reuter, in: Classical and Quantum Dynamics, Springer, Berlin, 1996, pp. 75–117.
[8] R. Pérez, M.C. Payne, I. Štich, K. Terakura, Phys. Rev. Lett. 78 (1997) 678.
[9] R. Pérez, I. Štich, M.C. Payne, K. Terakura, Phys. Rev. B58 (1998) 10,835.
[10] J. Israelachvili, Intermolecular and Surface Forces, Academic, London, 1992.
[11] T. Uchihashi, Y. Sugawara, T. Tsukamoto, M. Ohta, S. Morita, M. Suzuki, Phys. Rev. B56 (1997) 9834.
[12] R. Erlandsson, L. Olsson, P. Martenson, Phys. Rev. B54 (1996) R8309.
[13] J. Tóbik, I. Štich, R. Pérez, K. Terakura, Phys. Rev. B, (1999) 11639.
[14] S.H. Ke, T. Uda, R. Pérez, I. Štich, K. Terakura, Phys. Rev. B, (1999) 11631.
[15] M.C. Payne, M.P. Teter, D.C. Allan, T.A. Arias, J.D. Joannopoulos, Rev. Mod. Phys. 64 (1992) 1045.
[16] J.P. Perdew, J.A. Chevary, S.H. Vosko, K.A. Jackson, M.R. Pederson, D.J. Singh, D. Fiolhais, Phys. Rev. B46 (1992) 6671.
[17] Y. Sugawara, M. Ohta, H. Ueyama, S. Morita, Science 270 (1995) 1646.
[18] H. Ueyama, M. Ohta, Y. Sugawara, S. Morita, Jpn J. Appl. Phys. 34 (1995) 1086.